

Data collection from LoRaWAN sensor network by UAV gateway: design, empirical results and dataset

Gianmarco Canello^{*†}, Silvia Mignardi[†], Konstantin Mikhaylov^{*}, Chiara Buratti[†], Tuomo Hänninen^{*}

^{*}Center for Wireless Communications, University of Oulu, Finland, email: firstname.lastname@oulu.fi

[†]DEI, University of Bologna, Italy, email: {silvia.mignardi, c.buratti}@unibo.it

Abstract—Collecting data from Internet-of-Things (IoT) devices, especially the variety of sensors dispersed in the environment, is an increasingly important and difficult task. Several long-range radio-access technologies, such as low-power wide-area networks (LPWAN) and specifically LoRaWAN, have been proposed to address this challenge. However, until now, the key focus of the related studies has been on static terrestrial LPWAN deployments. In this study, we depart from this vision and investigate the practical feasibility and performance of a LoRaWAN gateway (GW) on a flying platform, specifically - an unmanned aerial vehicle (UAV). The key contributions of this study are (i) the design and field-testing of a packet-sniffer-based mobile LoRaWAN GW prototype, allowing collection of the data from LoRaWAN networks, including the already deployed ones; (ii) the open-publication of the data collected during our experimental campaign in the 426 LoRaWAN sensor node network of the University of Oulu illustrating the performance of different drone trajectories; (iii) the initial results of the system’s performance analysis, revealing some interesting trends and setting goals for further studies, and pinpointing the lessons learned during the experimental campaign. Our empirical findings suggest that the Travelling Salesman Problem (TSP) trajectory is the most effective moving trajectory for the number of packets collected and the average energy consumed per packet collected.

Index Terms—LoRaWAN, UAV, IoT, experiment, trajectory, non-terrestrial, field test, packet delivery, dataset, drone

I. INTRODUCTION

The number of Internet-of-Things (IoT) applications and devices is growing incredibly fast, supported by the progress in underlying technologies. Over the past years, substantial efforts have been invested in increasing the coverage and enabling the operation of IoT applications in remote areas. This has brought to the stage several radio access technologies featuring a combination of long-range communication and low IoT node energy consumption – the low-power wide area networks (LPWAN). Of these, LoRaWAN is quite popular [1] due to its flexibility, relatively simple design, and ease of use.

However, even though LoRa modulation underlying LoRaWAN can enable communication links with the length of several kilometers (and dozens of kilometers opportunistically), these do not provide an ultimate solution to enable ubiquitous connectivity for IoT. To offer just two illustrative examples: (i) even today, there are still many use cases in the regions lacking terrestrial infrastructure (e.g., in natural reserves, rural and Polar areas); (ii) there are some emergency and event-triggered applications and services. An illustrative example of the latter is a forest wildfire extinguishing case, where IoT sensors deployed on the trees or around them can

be used to detect the start, predict the propagation and ensure the extinction of fire.

Therefore, addressing this challenge as well as the need for increasing the reliability of IoT data collection (e.g., in case of energy blackouts affecting terrestrial infrastructure) in this paper, we report and advocate the employment of IoT radio infrastructure deployed on a mobile platform – an unmanned aerial vehicle (UAV). Compared to the state-of-the-art, the key novelties of our work are: (i) we discuss and report the design of a UAV-based LoRaWAN gateway (GW) prototype, which can be used either standalone or to complement an existing network; (ii) we report field trials conducted with the instrumented UAV LoRaWAN GW, during which we employed it to collect data from 426 LoRaWAN sensors scattered inside the University of Oulu as a part of Smart Campus initiative. Note that in this paper, we detail the experiment procedure and pinpoint just some selected results related to the instrumentation and operation of a flying LoRaWAN GW (e.g., the effect of the different trajectories on data collection performance). At the same time, we open-publish the data collected during the experiments for further use and to enable a more detailed analysis by the community.

The remainder of the paper is organized as follows. Section II discusses the state-of-the-art. Section III details the UAV GW design and describes the working environment, the trajectories and experiment procedures. Section IV presents the selected results and Section V concludes the paper, summarizing the lessons learned and prospective future steps.

II. RELATED WORKS

Given this work’s emphasis, we focus on the studies implying the use of a UAV-based LoRaWAN GW for collecting data from sensors scattered in the environment. These studies can be classified into two main categories based on the methodology. In the former, simulations or analytic methods are used, while the latter develop and use a real-life prototype and field tests. In Table I we summarize the contributions of the different papers, and below, we discuss them in more detail. In the rightmost column with N_d we show how many End Devices (EDs) were involved in the experiments.

First, we will briefly discuss the selected works belonging to the former category. Zorbas et al. [3] focused on energy efficiency and packet collection success rate: they modified the classical ALOHA transmission policy to introduce a more efficient synchronized time-scheduled transmission mechanism

TABLE I
RELATED WORKS

Ref.	Obtained results	Prototype	N_d
[2]	Design, implementation, and evaluation of an architecture for enhancing LoRaWAN deployments by employing a LoRa-drone GW	Yes	7
[3]	Developed a new transmission policy introducing a synchronized time-scheduled transmission mechanism to eliminate packet collisions	No	n.a.
[4]	Simulations show that adopting a flying LoRaWAN GW reduces the mean energy consumption of the EDs by up to 59%	No	n.a.
[5] - [6]	Developed and realized lab tests as well as an experiment of a flying LoRaWAN GW equipped with a simulated satellite connection	Yes	2
[7]	Obtained an analytical model that can be used to configure the path of the drone to guarantee a given probability of collecting LoRaWAN sensor data	No	n.a.
[8]	Developed a prototype where LoRaWAN is used on a drone to wake up high power 5-GHz transmitters on the ground	Yes	1
[9]	Simulations and financial analysis of a prototype drone tasked with charging LoRaWAN sensors placed in a remote location proved to be advantageous compared to manually replacing all sensors' batteries	No	n.a.

and eliminate packet collisions. They achieved 0% packet collisions through simulations in an environment populated by 80 devices. Tiurlikova et al. [4] focused on the energy efficiency aspect of adopting a flying LoRaWAN GW in the network, showing through simulations that a UAV-based GW can reduce the mean energy consumption of EDs for communication in the network by up to 59%. In Caruso et al. [7], a theoretical model is formulated to understand analytically how close a UAV that uses a LoRa radio needs to fly over the sensors to achieve a certain quality of data collection. The results can be used to determine the layout of the sensors on the ground, the type of drone to utilize, and the path shape that needs to be followed together with the battery size of the aircraft. A quite different approach to the use of drones for LoRaWAN networks is proposed in Tiurlikova et al. [9], where a drone equipped with wireless power transfer is evaluated as a means to replenish the batteries of all the LoRaWAN sensors of a remote deployment. The paper carries out feasibility and financial sustainability simulations comparing this approach with manual battery servicing.

Next, we focus on the second class of papers, where a real-life prototype is reported. So far, we have found only four such studies. In their work, Zhang et al. [8] adopt the LoRa technology as a wake-up signal for a 5-GHz transmitter for application data transfer. Note that although the authors used LoRa-modulated signals, the communication does not follow LoRaWAN specifications. The works by Marchese et al. [5], Moheddine et al. [6], and Gallego-Madrid et al. [2] focus on adopting the UAV to extend the coverage of the LoRaWAN network; they both develop a working prototype. In [5] and [6], the UAV is equipped with a LoRaWAN GW and a simulated satellite backbone connection. Experiments were carried out using just two sensors placed 100 meters apart on an open field while the drone moved in a random pattern at an altitude of 20 meters. Results for signal strength and energy consumption for lab tests and drone flights are compared; moreover, in [6], the authors compare the difference

in performance between the drone acting as a data mule and a simulated satellite connection. In study [2], the prototype was designed to overcome the problematic orography of the area where sensors were placed, which did not allow the GW to collect data from all the sensors. In the field-trial phase, the authors employed seven EDs with one ground GW and two locations where the UAV-equipped GW hovers. The results for packet delivery ratio (PDR) are reported in the paper.

As seen from the discussion above, the number of experimental studies on the use of UAV-based LoRaWAN GW is low, as is the scale of their experimental campaigns. Notably, none of the referenced works, to the best of our knowledge, provides an openly accessible dataset. In contrast, in this study, we investigate the case when a flying LoRaWAN GW collects the data from the already deployed massive LoRaWAN network, composing more than 400 sensors. Also, during our experiments, the packets sent by LoRaWAN sensors were collected simultaneously by a terrestrial GW and the UAV-based mobile GW. Therefore, our results allow to compare the performance of the two deployment types and shed some light on the added value of a flying GW within a LoRaWAN network that is already served by a static GW. Finally, we report the experimental results for five different drone trajectories. To our knowledge, such results are not yet available in the literature.

III. EXPERIMENT DESIGN AND ENVIRONMENT

A. Experiment environment

The Oulu University campus is located in the Linnanmaa district; it covers an area larger than 180 000 m^2 . Inside the university, there are several active LoRaWAN sensor networks. The most extensive one and of primary interest for this work belongs to the Smart Campus initiative; it includes 426 active sensors (Elsys.se model ERS [10]), each transmitting once every 900 seconds (more information, including the map of the sensors, is available from [11] and [12]). The deployed sensors measure and communicate temperature, humidity, light, motion, CO₂ concentration, and sound volume data. The uplink transmissions of the different sensors are not synchronized.

The LoRaWAN network is served by one static GW (model: Multitech Conduit) equipped with an omnidirectional antenna (biconical D100-1000 by Aerial) mounted to an external mast over the university rooftop 28 meters above the ground level. Data captured by this GW is streamed to InfluxDB, a time series database, and visualized through the Grafana platform. The Smart Campus project makes data openly available through periodic publications [11].

B. Flying gateway platform design

Given that the network discussed in the previous subsection is already running and collecting data used by several applications, we aimed at a solution that would not alter the present setup when designing our testbed and experiments. This requirement posed two major challenges. The former originated from the fact that the already deployed sensors were configured to use the over-the-air activation (OTAA) procedure defined by LoRaWAN specifications. Due to this, the sensors'

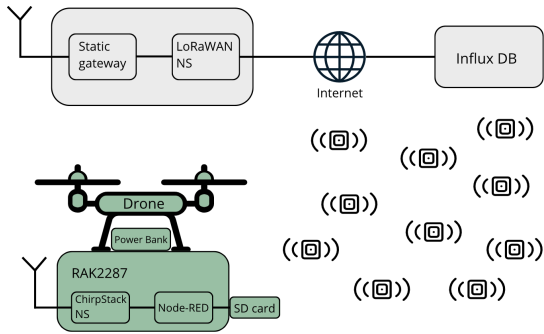


Fig. 1. The structure of the set-up for the field trials.

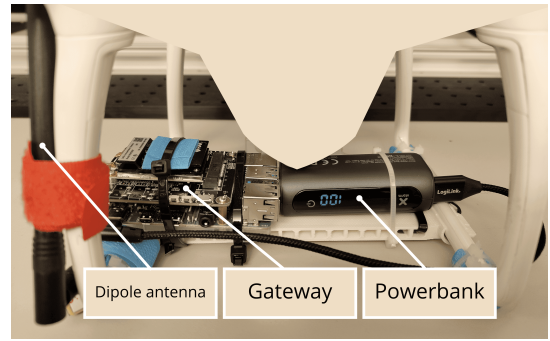


Fig. 2. Photo of the aerial LoRaWAN GW used in field trials.

security keys were generated by the network server (NS) for each new connection of a device. Given that the sensors can occasionally reconnect or reboot for various reasons resulting in keys being changed, this made pre-storing the keys on the UAV-based GW impossible. Meanwhile, enabling a stable backbone wireless connection between the GW on a mobile UAV and a ground-based NS also appeared to be extremely challenging, especially while complying with the Finnish frequency regulations, which prohibit the use of any mobile network equipment on any aerial vehicles, including UAVs.

After analyzing the pros and cons, we opted to implement the UAV GW as a "packet sniffer" – it receives and logs in its memory all the LoRaWAN packets it observes, but the analysis of the data and their interpretation is made offline after the flight. However, on the positive side, this allows a fully-autonomous and independent operation of the UAV-based LoRaWAN GW. Notably, this approach does not introduce new security vulnerabilities since the drone, even if intercepted or lost, does not have the keys to decrypt network or application data. Also, it is very scalable since the drone does not require keys, can collect packets from different LoRaWAN networks simultaneously, and does not introduce extra signaling. On the negative side, this approach does not enable the implementation of acknowledged transmissions (these are not used in the Smart Campus network) and introduces a time delay before the data are received and decoded. Therefore, this design approach is prospective for non-latency-critical applications only.

Figure 1 shows the overall testing environment. The data pipeline of the University of Oulu fixed LoRaWAN network is shown at the top. The static GW sends the received packets to the NS, which is connected to the Internet and forwards the data to InfluxDB. From there, all the data needed for the analysis can be downloaded in a *csv* format. On the bottom, the structure and the pipeline for the flying GW setup are illustrated. The drone is carrying the battery-powered (65160 J) RAK2287 dev kit [13], connected to an HWR Series ½-wave center-fed dipole antenna [14]. The system hosts a ChirpStack NS locally. Node-RED stores all the packets captured by the mobile GW onto a Secure Digital card. Notably, both GWs can simultaneously receive packets from the sensor nodes.

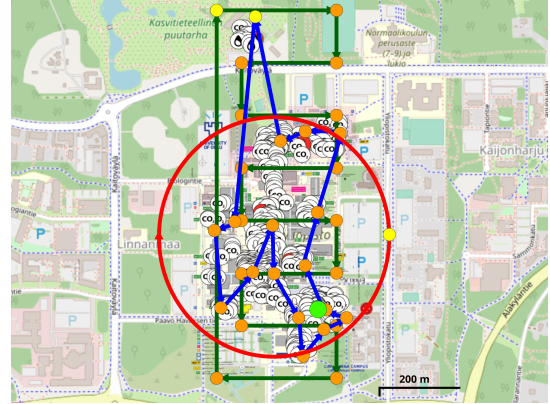


Fig. 3. The trajectories overlaying the University of Oulu map. The TSP trajectory is represented in blue, the Scan trajectory is green, and the Orbit is red. Yellow dots are the starting/ending points. The larger lime-colored dot represents the location of the static ground LoRaWAN GW's antenna.

C. Trajectories

The major benefit a drone offers – is its mobility. Unfortunately, no previous experimental work studied the effect of the trajectory on communication performance; thus, we carried out such study in this work. Specifically, we considered the following drone mobility patterns (i.e., the trajectories):

- The first two scenarios implied the drone hovering in the air stationary. The first hovering spot was above the *K-means* centroid of all EDs' locations; the second hovering location was above the stationary GW's antenna position. These trajectories are further referred to as "Mid" and "Actual", respectively.
- The third scenario (the "Orbit") implied the circular motion of the UAV centered at the *K-means* centroid of all EDs' positions. An arbitrary radius of 250 meters was chosen to cover the whole university area.
- For the fourth case a conventional drone scan (denoted "Scan") trajectory was generated to cover the approximate area occupied by the university buildings (i.e., 251 m width, 725 m length).
- Finally, for the fifth case, we have employed the Travelling Salesman Problem [15] (denoted "TSP") solution to optimize the drone movement. A number of reference points (i.e., coordinates in the campus map) were identi-

fied, starting from all sensor node locations. As they are many, the positions of sensor nodes were first grouped into clusters. The *K-means* algorithm [16] was selected as a clusterization method for the sensor nodes, obtaining 17 cluster center locations that are then used as reference points for the movement. The final trajectory was obtained by solving an NP-hard combinatorial optimization problem to find the shortest closed tour through the set of reference points.

All the different trajectories are illustrated in Fig.3. A flight automation software was employed to configure the drone to follow the trajectories with high fidelity. The flight altitude was set to 45 meters above ground in all experiments to avoid possible obstacles along the path; for the trajectories involving the drone moving, its speed was set to constant 5 m/s. In the future, other heights and speeds will be considered.

D. Experiment routine

Several considerations were made to ensure the safety of people, equipment, and the environment. First, the weather conditions (e.g., temperature, humidity, wind speed, and visibility) and the crowdedness of the area were analyzed before each flight on site. The experiments were executed outside business hours in the late evenings to minimize the number of people around. Note that the experiments were conducted in June 2022, when the daylight duration in Oulu exceeds 20 hours, thus enabling good visual conditions in the evenings.

Before the start of each flight, the home point location was configured at the drone to allow its autonomous safe return in case of communication failure or other unforeseen circumstances. Also, as the longest trajectories required a large percentage of the drone battery, it was in the best interest to take off as close as possible from the start of the trajectory. Special software has been used to automate the flight of the pre-configured trajectories. All flights were carried out under human supervision, maintaining a visual line of sight between the pilot and/or a dedicated observer and the drone at all times. After every landing, the drone and the GW were powered off to reset the packet counter, creating a clear separation of the data collected during the different flights. The results were collected by executing four flights for each trajectory.

E. Data analysis

During the experiment, several datasets were collected. First, the LoRa packets received by the drone were stored in a *txt* file on the GW's memory card. Second, the LoRa packets received by the stationary GW during the experiments were extracted from the database, downloaded and saved in a *csv* file format, and later transferred into the data analysis software. Third, the flight log of each run was also saved, allowing to check the integrity of the trajectories against the designed ones uploaded into the flight automation software and enabling tracking of the change of the drone's position in time. The collected data composes of:

- **For the flying GW:** time in epoch format, packet counter from the last boot of the GW, data packet (consisting of

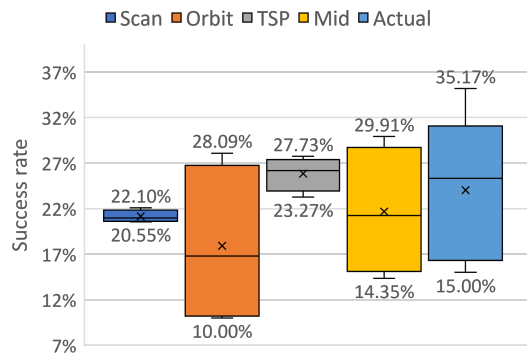


Fig. 4. PDR for different trajectories. The confidence interval is delimited by the black lines on the top and bottom of each trajectory, the median value represented as a horizontal line, and the average is shown as a black cross.

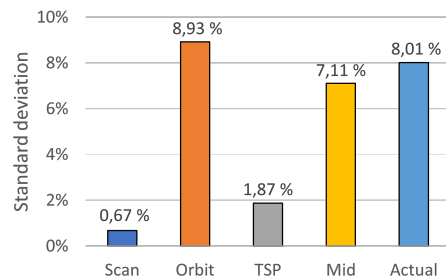


Fig. 5. Standard deviation for PDR. The trajectories are placed and colored similarly to the previous figure.

an unencrypted header that includes the sensor's network address, packet counter and other relevant information, while the rest of the packet is the encrypted payload);

- **For the fixed GW:** time in epoch format, sensor's network address, sensor's identifier (EUI), frame counter, data rate, channel, frequency, radio signal strength indicator (RSSI), signal-noise ratio (SNR), and packet size;
- **For the trajectories and drone position:** latitude, longitude, and altitude for each data point of the drone trajectory, speed of the drone, its orientation, etc.

The data sets and metadata can be downloaded from [17]. The data file, containing the analysis of captured packets, is organized as follows: there is a worksheet for every type of trajectory containing all the field trials. In each of them, the data is laid out in columns. On the left side, there is all the information downloaded from the drone; in the middle, a gold-colored column indicates the packet match between the stationary GW and the drone. On the right side of this column, we placed the data downloaded from the database of the fixed GW. Packet matches are highlighted by showing the row number containing the packets that match the MAC Header (MHDR) from the fixed GW data. All the trajectory logs are provided in the form of *ods* and *gpx* files and can be imported into visualization tools such as Google Earth.

Since this study's key focus is investigating the performance of a UAV-based LoRaWAN GW, we have analyzed the data

on the LoRa PDR. Specifically, we have used the stationary GW’s packet log to figure out the Device Address (DevAddr) used by the LoRaWAN sensors during the flights. Then, we analyzed the contents of the frame (FHDR) and the media access (MAC) MHDR headers, which are sent unencrypted in LoRaWAN, for the packets received by the drone-based GW to identify the uplink data packets and the sensors they originate from. Furthermore, we used the frame counter (FCnt) to distinguish the packets originating from the same sensor.

Next, we categorized all the packets received by the UAV-based GW into four categories. First, we identified the packets received by both GWs (“Cat.Dbl”). Second, we determined the packets with valid DevAddr and counter that the stationary GW did not receive (“Cat.UAV”). Third, we specified the packets with the DevAddr not assigned to any sensor in our network as external interferences (“Cat.Int”). Finally, we grouped all service packets (i.e., any LoRaWAN packet types other than uplink) or the packets having incorrect structure (i.e., a not user-data) packet (“Cat.Oth”).

IV. RESULTS

Since it was only possible to conduct four flights for each trajectory due to adverse weather conditions, the statistical relevance of the results should be carefully considered. Nonetheless, some trends and lessons learned can be identified.

This study’s main parameter of interest was the PDR from ground sensors to the drone GW. This statistic was computed by dividing the number of all packets collected by the drone (i.e., the number of packets in Cat.UAV and Cat.Dbl) by the total number of packets sent by the sensor nodes during the same time interval. The PDR for each trajectory is depicted in Fig. 4, and its standard deviation is shown in Fig. 5. The first thing to note is the relatively low PDR to the mobile GW. We expect the possible reason for this result is the used antenna – the half-wavelength dipole- attached to one of the drone’s legs (see Fig.2). Currently, we are conducting further investigations into this matter and taking measures to improve the performance by designing a specialized antenna. Nonetheless, since all the trajectories have been affected equally, we consider that their performance can still be compared fairly.

Comparing the PDR for the different trajectories, on average, the TSP tends to be the most successful. Moreover, considering the average and median values of the PDR, the results of TSP surpass that for static drone positions; however, considering the confidence interval, the stationary positions may outperform the TSP. The performance of Scan and Orbit trajectories was substantially lower. Interestingly, the Orbit and static trajectories were characterized by the high variance of the results. Though we are still investigating this phenomenon, we expect that it may be caused by the drone’s orientation, which was not explicitly configured in our tests.

Figure 6 illustrates how much interference the flying GW was exposed to during the experiments. The interference rate was computed by dividing the total number of packets in Cat.Int and Cat.Oth by the total number of packets the drone received. The figure clearly shows that a large percentage

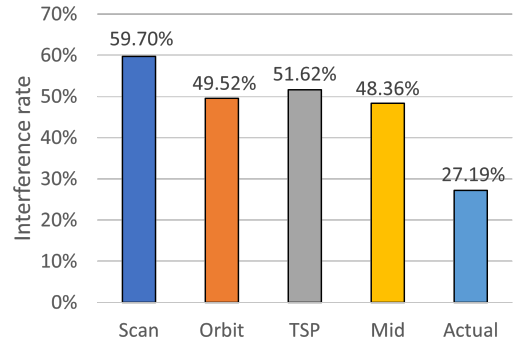


Fig. 6. Average interference rate for different trajectories

TABLE II
EXPERIMENTS STATISTICS

Traj.	Number of packets				T_{flight}	E_{tot}	E_{pkt}
	min	max	total	avg	avg (s)	avg (J)	avg (J)
Scan	181	197	755	188.75	654	1785.42	44.73
Orbit	40	87	249	62.25	326	889.98	79.77
TSP	127	146	542	135.5	462	1261.26	36.03
Mid	59	134	389	97.25	427	1165.71	55.28
Actual	46	161	410	82	427	1165.71	59.18

T_{flight} is the average flight time for each trajectory, E_{tot} is the total energy consumed by the GW for each trajectory (computed as average GW power consumption multiplied by T_{flight}), E_{pkt} is the average energy consumed by the GW to receive one packet from the target network (Cat.UAV & Cat.Dbl).

of packets received by the flying GW originated from the devices extraneous to the university network. This testifies that the testing environment is highly congested; moreover, it is noticeable that the Actual trajectory has a lower interference rate than the others. This could be because the hovering point is placed over the southern part of the university, where a lower number of buildings and, thus, fewer sensors are present.

Finally, Table II summarizes the statistics on the number of packets received by the mobile GW for the different trajectories and the average flight times (which also correspond to the energy consumed by the drone). The minimum (min), maximum (max), total, and average (avg) numbers for different flights are shown. In the three rightmost columns, we report an assessment of the average energy consumption for the GW mounted on the drone. We measured the average power consumption to be 2.73 W (the consumption of the stationary GW is more than three times higher - 9.78 W). This analysis made it possible to compute E_{pkt} , the average energy consumed by the flying GW to receive a single packet from the Smart Campus network. This term indicates the efficiency of each trajectory; concerning this metric, the TSP outperforms the Scan, with the second-best figure by about 20%.

V. CONCLUSIONS

The use of non-terrestrial infrastructure for improving the performance of IoT data collection has a strong potential. Therefore, in this paper, we reported the design and results

of an experimental study focusing on collecting data from an extensive LoRaWAN sensor network by a drone-based GW. The novel contributions of this work are: (i) the design and field-testing of a packet-sniffer-based mobile LoRaWAN GW, allowing non-intrusive and autonomous collection of the data from LoRaWAN networks, including the already deployed ones; (ii) the data collected during our experimental campaign illustrating the performance of the different drone trajectories, which we publish open-access; (iii) the initial results of the system's performance analysis, revealing some interesting trends and setting goals for further studies. To the best of our knowledge, none of the previous studies has (i) experimentally investigated drone-based data collection from a network composed of more than 400 nodes, (ii) reported the data both for static and mobile GWs operating simultaneously, (iii) studied the effect of the trajectory, and (iv) openly published the data from on-field experiments. Although the presented node deployment is specific to the University of Oulu, we consider that the obtained results can be further generalized. For example, the methodology for building the TSP trajectory, carrying the flights and handling the data processing can be employed for other use cases and studies. More experimental flights are needed to increase the statistical relevancy of the presented results, but preliminary empirical findings suggest that the TSP trajectory is the most effective between the moving trajectories concerning the PDR.

However, we have faced several challenges which affected the obtained results. First, the weather and time constraints limited the number of flights. Second, the post-experiment analysis of the results revealed that the overall PDR for the mobile GW was substantially lower than the static GW. We expect that the primary reasons for it are the low performance of the used non-UAV-optimised antenna and the fact that the orientation of the drone during the flight was not explicitly controlled. Nonetheless, we do not expect that this issue invalidates the results of our reported trajectory comparison since all trajectories were affected equally. We are currently approaching these problems by characterizing the antenna performance, developing a specialized antenna, and investigating the effect of the drone's orientation on communication performance. However, we would like to stress the importance of properly selecting the antenna and its positioning on the drone as one of the lessons learned and crucial factors related to the practical performance of IoT data collection by a drone.

Among the other aspects which we consider worth investigating are: (i) further trajectory optimization (also using machine-learning-based methods, both for standalone drone operation and accounting for the presence of static GWs), (ii) adaptation of the radio parameters (e.g., LoRa spreading factor) for data collection by drones, (iii) development of the different architectures for sensor data collection by a drone (e.g., from real-time data decoding/streaming to fully autonomous drone operation). The prospective directions for further analysis of the data which we have already collected and made publicly available include: (i) analyzing the effect of the speed, distance, and orientation of the drone towards

a sensor on its packet's delivery success probability, (ii) exploring which of the trajectories is more efficient considering the drone operation not as standalone (as we have done in this paper), but in cooperation with a stationary GW (i.e., to maximize the number of unique packets received by both static and mobile GW), (iii) studying the impact of the modulation-coding scheme and transmit power used by different nodes.

VI. ACKNOWLEDGEMENTS

The research was supported by the Academy of Finland projects FIREMAN (decision 348008), MRAT-SafeDrone (341111), Robomesh (336060) and 6G Flagship program (346208). The study was also supported by COST Action CA20120 INTERACT. We also thank Mr. Janne Rajala, the chief pilot of CWC, for his support during the experimental phase of the project.

REFERENCES

- [1] IndustryARC. [Online]. Available: <https://www.industryarc.com/Report/19424/lora-and-lorawan-devices-market.html>
- [2] J. Gallego-Madrid *et al.*, "Enhancing Extensive and Remote LoRa Deployments through MEC-Powered Drone Gateways," *Sensors*, vol. 20, no. 15, 2020.
- [3] D. Zorbas and B. O'Flynn, "Collision-Free Sensor Data Collection using LoRaWAN and Drones," in *Proc. Global Inf. Infrastructure and Netw. Symp.*, 2018, pp. 1–5.
- [4] A. Tiurlikova, N. Stepanov, and K. Mikhaylov, "Improving the Energy Efficiency of a LoRaWAN by a UAV-based Gateway," in *Proc. 11th Intern. Congr. Ultra Modern Telecommun. Control Syst. and Workshops*, 2019, pp. 1–6.
- [5] M. Marchese, A. Moheddine, and F. Patrone, "UAV and Satellite Employment for the Internet of Things Use Case," in *Proc. IEEE Aerospace Conf.*, 2020, pp. 1–8.
- [6] A. Moheddine, F. Patrone, and M. Marchese, "Comparison between UAV IoT solutions with and without satellite backhaul link," in *Proc. IEEE Aerospace Conf.*, 2022, pp. 1–8.
- [7] A. Caruso *et al.*, "Collection of Data With Drones in Precision Agriculture: Analytical Model and LoRa Case Study," *IEEE IoT J.*, vol. 8, no. 22, pp. 16 692–16 704, 2021.
- [8] M. Zhang and X. Li, "Drone-Enabled Internet-of-Things Relay for Environmental Monitoring in Remote Areas Without Public Networks," *IEEE IoT J.*, vol. 7, no. 8, pp. 7648–7662, 2020.
- [9] A. Tiurlikova, N. Stepanov, and K. Mikhaylov, "Wireless power transfer from unmanned aerial vehicle to low-power wide area network nodes: Performance and business prospects for LoRaWAN," *Int. J. Distributed Sensor Netw.*, vol. 15, no. 11.
- [10] ELSYS.se. [Online]. Available: https://elsys.se/public/datasheets/ERS_datashet.pdf
- [11] University of Oulu. [Online]. Available: <https://smartcampus.fi/oulu/>
- [12] R. Yasmin, K. Mikhaylov, and A. Pouttu, "LoRaWAN for Smart Campus: Deployment and Long-Term Operation Analysis," *Sensors*, vol. 20, no. 23, 2020.
- [13] RAKwireless. [Online]. Available: <https://docs.rakwireless.com/Product-Categories/WisHat/RAK2287-RAK5146-Pi-HAT/Datasheet/product-background>
- [14] Linx Technologies. [Online]. Available: <https://linxtechnologies.com/wp/wp-content/uploads/ant-868-cw-hwr.pdf>
- [15] E. Lawler, *The Travelling Salesman Problem: A Guided Tour of Combinatorial Optimization*, ser. Wiley-Interscience. John Wiley & Sons, 1985. [Online]. Available: <https://books.google.fi/books?id=qbFIMwEACAAJ>
- [16] S. P. Lloyd, "Least squares quantization in pcm," *IEEE Trans. Inf. Theory*, vol. 28, pp. 129–137, 1982.
- [17] University Of Oulu, CWC, "Data collection from smart campus lorawan sensor network by uav gateway: open dataset," <https://doi.org/10.23729/65afdfc0-cdda-4e69-8a63-05b9261b7328>, April 2023.